



ELSEVIER

Carbohydrate Research 308 (1998) 19–27

# Conformational differences between Fuc( $\alpha$ 1–3)GlcNAc and its thioglycoside analogue

Begoña Aguilera, Jesús Jiménez-Barbero \*, Alfonso Fernández-Mayoralas \*

*Departamento de Química Orgánica Biológica, Instituto de Química Orgánica, CSIC, Juan de la Cierva 3, 28006 Madrid, Spain*

Received 17 November 1997; accepted 5 March 1998

---

## Abstract

NOE measurements and molecular mechanics calculations have been performed to study the conformational behaviour of Fuc( $\alpha$ 1–3)GlcNAc and its thioglycoside analogue in solution. Experimental data show that, in contrast with the natural *O*-disaccharide, which is basically monoconformational, the *S*-analogue shows two conformational families, namely *syn* and *anti*.  
© 1998 Elsevier Science Ltd. All rights reserved

*Keywords:* NOE spectroscopy; Molecular mechanics calculations; Thiodisaccharides; Lewis antigens; Conformational analysis

---

## 1. Introduction

The sequence Fuc( $\alpha$ 1–3)GlcNAc is a principal constituent of Le<sup>x</sup>-bearing glycoconjugates, which play an important role in numerous biological phenomena. For instance, sialyl Le<sup>x</sup> tetrasaccharide has been shown to be recognized by E-selectin, a protein involved in the acute inflammatory process [1], and is often expressed in tumor cells and carcinomas [2]. Besides, we have reported [3] that some oligosaccharides structurally related to Le<sup>x</sup> are inhibitors of neural cell division. In order to prepare oligosaccharides that are more stable for in vivo experiments, we were interested in the synthesis of Le<sup>x</sup>-analogues with a sulfur atom linking the glucosaminyl and fucosyl moieties. It is known that *S*-linked oligosaccharides are

resistant to glycosidase-catalysed hydrolysis, and more stable at acidic pH than the corresponding *O*-glycoside [4].

An important aspect in understanding the molecular bases of oligosaccharide-mediated biological processes is the determination of the conformational flexibility around the interglycosidic bonds. Therefore, it is important to determine whether the conformational characteristics of the natural compounds are reflected in the thio-oligosaccharide analogues. We have carried out a comparative conformational study of propyl *O*-( $\alpha$ -L-fucopyranosyl)-(1→3)-2-acetamido-2-deoxy- $\beta$ -D-glucopyranoside (**1**) and its *S*-interglycosidic analogue **2**, using NMR spectroscopy and molecular mechanics calculations. Thus, NOE measurements and molecular mechanics calculations [5,6] have been performed to estimate the probability distribution of conformers of both analogues in solution. Experimental data show that, in contrast with the natural

---

\* Corresponding authors. Fax: +34-1-5644853; e-mail: iqojj01@pinar1.csic.es

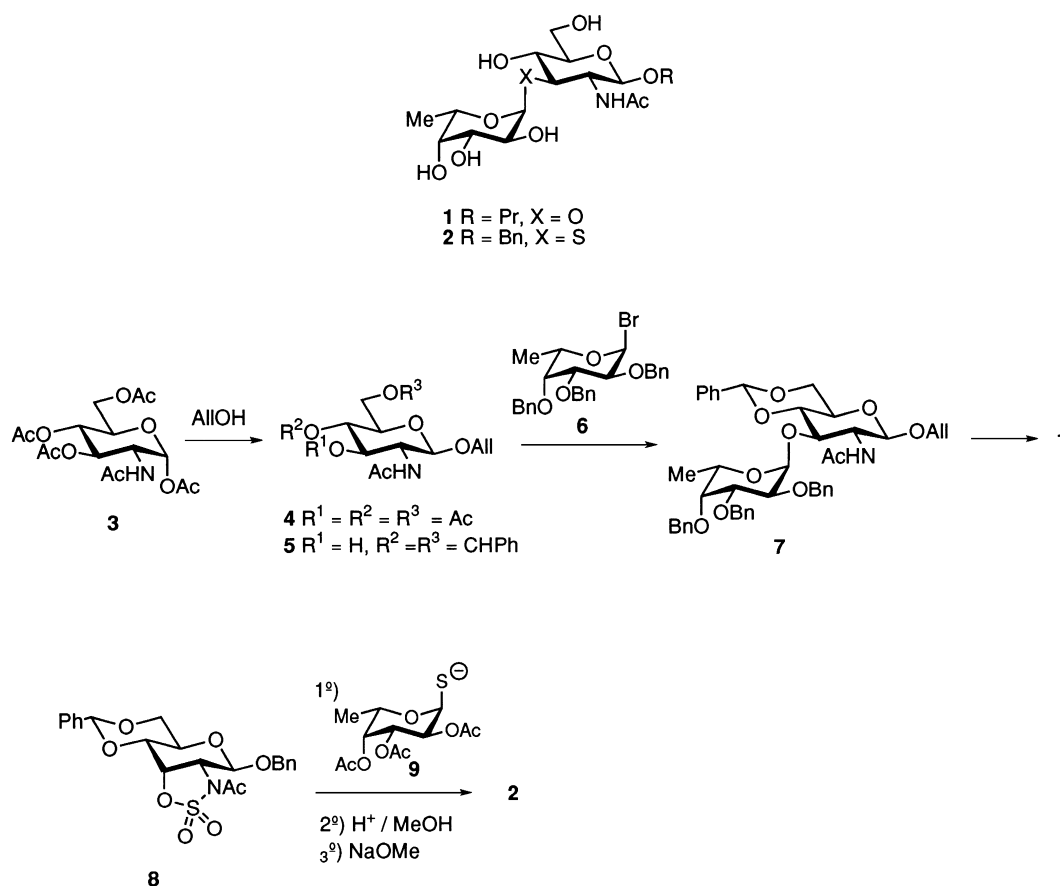
*O*-analogue, which is basically monoconformational, the *S*-disaccharide presents two conformational families in solution, namely *syn* and *anti*.

## 2. Results and discussion

**Synthesis.**—The synthesis of **1** started from peracetylated  $\alpha$ -glucosamine **3** following procedures for related disaccharides [7] (Scheme 1). Glycosylation of **3** with allyl alcohol using  $\text{SnCl}_4$  as acid promotor gave **4**, which after deacetylation and subsequent benzylidenation provided alcohol **5**. Treatment of **5** with fucosyl bromide **6**, in situ, prepared from ethyl 2,3,4-tri-*O*-benzyl-1-thio- $\beta$ -L-fucopyranoside [8], in the presence of  $\text{Bu}_4\text{NBr}$  afforded the fully-protected disaccharide **7** in 79% yield. Catalytic hydrogenation of **7** provided the desired disaccharide **1**.

The synthesis of thio-disaccharide **2** was recently reported [9]. Briefly, **2** was obtained by regioselective opening of the cyclic sulfamidate **8** with fucose **9**, followed by deprotection steps.

**Conformational analysis.**—**Molecular mechanics calculations.** The structures of **1** and **2** with the atomic numbering is shown in Scheme 1. Torsional angles around the glycosidic linkage are defined as  $\phi$  H-1'-C-1'-O(S)-C-3 and  $\psi$  C-1'-O-1'-O(S)-H-3. Figs. 1 and 2 show the adiabatic maps calculated from the respective relaxed energy maps for MM3\* (MM2\* for **2**) and AMBER\* force fields [10,11], using  $E=80$ . For **1**, both force fields predict two low energy regions, corresponding to the so-called *syn* and  $\Psi$ -*anti* regions [12,13]. The central *syn* region is fairly extended along  $\Psi$ , including both positive and negative  $\Psi$  values. Indeed, MM3\* predicts the existence of two different minima within this region which have been dubbed *syn*-A and *syn*-B conformers, respectively. The *syn* region heavily dominated the probability distribution since the central region is populated in more than 94%, independent of the force field used. In addition, the region around conformer *syn*-A (global minimum in both cases) with positive  $\Psi$  angles is populated between 63 (AMBER\*) and 76% (MM3\*). The geometries of the minima are very



Scheme 1.

similar for both force fields, with minor differences around the glycosidic linkages (Table 1, Fig. 3), and are in accordance with the exo-anomeric effect [14]. The potential energy surfaces obtained are

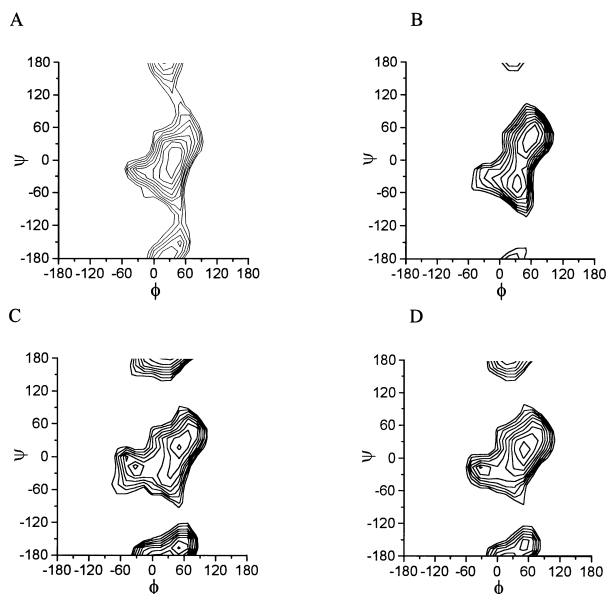


Fig. 1. Comparison of the adiabatic maps calculated by using AMBER\* (a,c), MM3\* (b) and MM2\* (d) force fields for compounds **1** (a,b) and **2** (c,d). Levels are drawn every 2 kJ/mol.

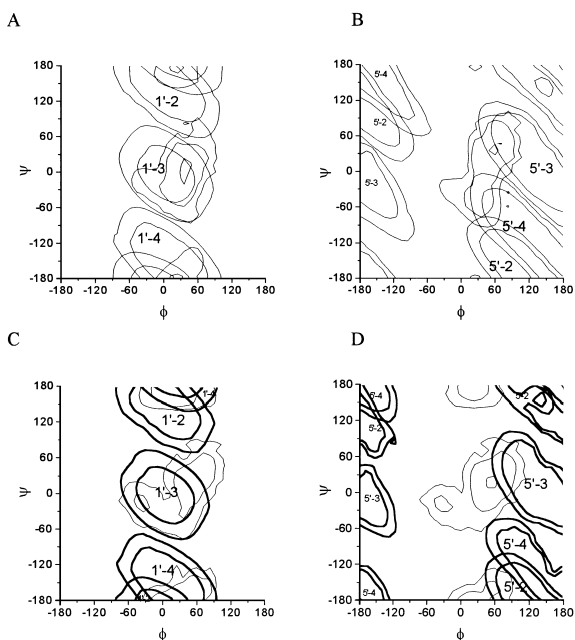


Fig. 2. Comparison of the probability distribution maps calculated by using AMBER\* (a,c), MM3\* (b) and MM2\* (d) force fields for compounds **1** (a,b) and **2** (c,d). Levels are drawn at 10, 1, and 0.1% probability. Relevant proton-proton short distances are labelled and superimposed onto the maps. Contour levels are drawn at 2.0 and 3.5 Å.

also similar to that obtained previously for the same disaccharide using the regular MM3 force field [15]. With this force field, the global minimum conformation also corresponds to the *syn*-A conformer with  $\Phi/\Psi$  values of 45/16. It is interesting to mention that, with both MM3\* and AMBER\* force fields, the obtained global minima for this disaccharide also corresponds satisfactorily to the conformation found for the Le<sup>x</sup> trisaccharide in the solid state [16] ( $\Phi/\Psi$  40/15 and 50/12, for the two independent molecules which exist in the crystal).

The situation is different for **2**. In this case, both AMBER\* and MM2\* force fields predict again the two low energy regions (Figs 1 and 2), similar to those obtained above for the natural compound, and again the geometries of the minima are closely related (Table 2, Fig. 4). AMBER\* and MM2\* predict, however, different global minima, and rather distinct population distributions. Using MM2\*, the most populated region is that corresponding to the central minimum (*syn*,  $\phi$ ,  $\psi$  = 55, 16), and the global minimum is the *syn*-A

Table 1

Ensemble average populations (calculated from the relative steric energy values) of the low energy regions of the *O*-disaccharide.  $\Phi/\Psi$  points are assigned to any of the basic regions based on proximity

min	AMBER*		MM3*	
	$\phi$ , $\psi$	Pop. (%)	$\phi$ , $\psi$	Pop. (%)
<i>syn</i> -A	42, 20	94.2	61, 43	76.4
<i>anti</i>	34, 169	5.8	35, 170	0.3
<i>syn</i> -B	Converges to <i>syn</i> -A	—	34, -49	23.3

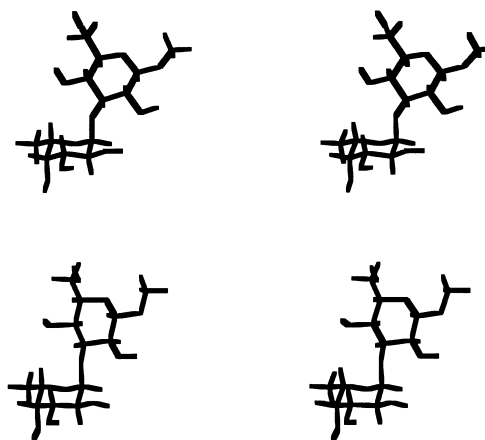


Fig. 3. Stereoscopic view of the global minima of **1**: (A) conformer *syn*-A, AMBER\*; (B) conformer *syn*-A, MM3\*.

conformer. The population of the *anti* region now amounts to 14%. AMBER\* locates the most populated region (49%) around the global minimum, in this case the so-called *anti* conformer [12]. Nevertheless, the addition of *syn-A* and *syn-B* conformers is basically equal to those populating the *anti* valley.

There are proton–proton short distances which give characteristic NOEs which may help in deducing the existence of the three different regions of the conformational map. Consequently, these NOE intensities will be sensitive to their respective populations. For both compounds, H-3–H-1' defines the central *syn*-region (both A and B conformers), while H-3–H-5 is sensitive to population around region *syn-A*. On the other hand, H-2–H-1' and H-4–H-1 are exclusive for the *anti* conformation. Therefore, the existence of the different conformational families in solution could be detected by the presence of these NOEs. Fig. 2 shows the relevant interresidue proton distances for **1** and **2**, superimposed on the probability distribution maps.

*NMR results.* Measurements of nuclear Overhauser enhancements [17] were made and subse-

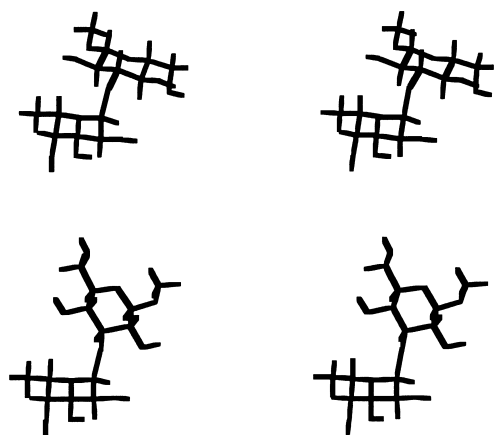


Fig. 4. Stereoscopic view of the major minima of **2**: (A) conformer *anti*, AMBER\*; (B) conformer *syn-A*, MM2\*.

Table 2

Ensemble average populations (calculated from the relative steric energy values) of the low energy regions of the *S*-disaccharide.  $\Phi/\Psi$  points are assigned to any of the basic regions based on proximity

min	AMBER*		MM2*	
	$\phi, \psi$	Pop. (%)	$\phi, \psi$	Pop. (%)
<i>syn-A</i>	56, 27	43.9	55, 16	78.8
<i>anti</i>	47, 177	49.4	39, 170	14.5
<i>syn-B</i>	-32, -25	6.7	-27, -25	6.7

quently compared to those obtained from the previously mentioned force field calculations. An effective average correlation time of 45 ps at 310 K was estimated from the matching of the experimental NOEs obtained for two intrasidue proton pairs to those theoretically predicted. No overlapping between key protons was found, thus facilitating the NOE analysis (Fig. 5).

The experimental NOEs, compared to those calculated are collected in Tables 3 and 4. For **1**, both MM3\* and AMBER\* force fields produce a reasonable agreement between expected and observed NOEs. In particular, the matching produced by AMBER\* may be considered almost excellent, within experimental error. On the other hand, MM3\* predicts a H-3–H-5' NOE higher than the experimental one, which probably means that the actual population around minimum *syn-A* is smaller than that calculated, 76%, more in agreement with the AMBER\* value of around 60%. The H-3–H-1' intensity is fairly well reproduced by both force fields. On the other hand, AMBER\* predicts correctly the H-4–H-5 NOE. Taking into account all these data, the experimental NOEs could be explained by a population distribution similar to that proposed by AMBER\*, always with the *syn* and *anti* regions populated in about 90–95 and

Table 3

Experimental and calculated ( $\tau_c$ , 45 ps) normalized NOESY intensities (%) for the *O*-disaccharide at 310 K in D<sub>2</sub>O solution, at 500 MHz

Proton pair	Mixing time 300 ms		Mixing time 450 ms			
	Exp.	AMBER*	MM3*	Exp.	AMBER*	MM3*
H3–H1'	3.8	4.0	2.6	5.3	6.0	3.9
H2–H1'	0.9	0.1	0.4	1.3	0.2	0.8
H4–H1'	0.4	0.2	0.2	0.6	0.4	0.4
H3–H5'	0.2	0.1	1.5	0.5	0.1	2.3
H4–H5'	0.5	0.4	0.7	1.0	0.8	1.1

Table 4

Experimental and calculated ( $\tau_c$ , 45 ps) normalized NOESY intensities (%) for the *S*-disaccharide at 310 K in D<sub>2</sub>O solution, at 500 MHz

Proton pair	Mixing time 300 ms		Mixing time 450 ms			
	Exp.	AMBER*	MM2*	Exp.	AMBER*	MM2*
H3–H1'	2.4	1.5	2.1	3.2	2.3	3.2
H2–H1'	0.8	1.1	0.4	0.9	1.6	0.9
H4–H1'	1.0	2.7	0.9	1.6	4.0	1.4
H3–H5'	0.6	0.2	0.4	0.8	0.4	0.9
H4–H5'	0.8			0.5		

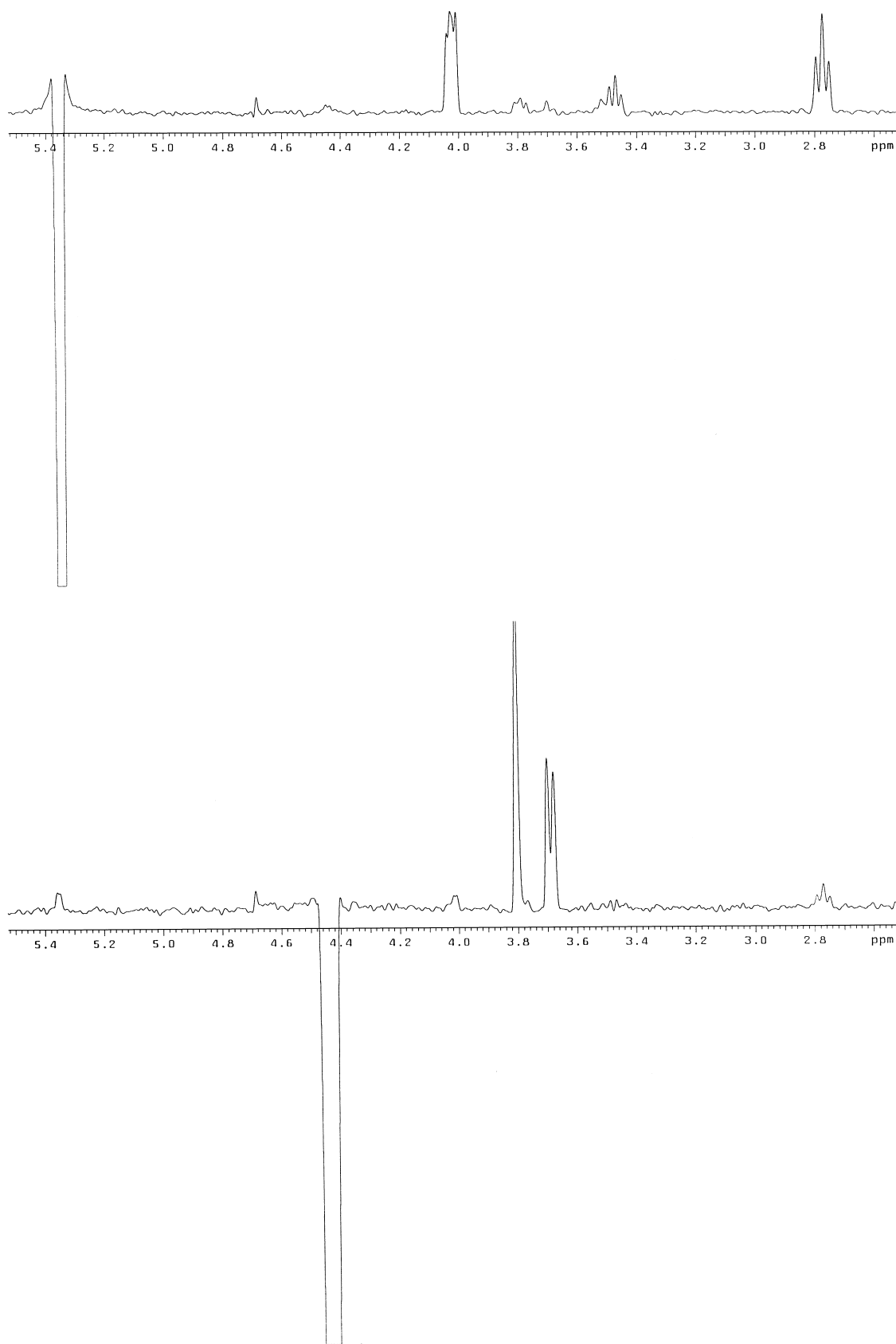


Fig. 5. 1D DPGNOE  $^1\text{H}$  NMR spectra of **2** at 500 MHz acquired with a mixing time of 450 ms.

5–10%, respectively. Similar results have been described for other disaccharides [13].

In the case of **2**, the experiments show a relative decrease of the H-3–H-1 NOE along with the corresponding increase of the H-2–H-1 and H-4–H-1 NOEs, a clear indication of a flow of population from the *syn* to the *anti* region, in comparison with the natural compound, **1**. Nevertheless, from inspection of Table 4, it is evident that the match between experimental and theoretical results is much better when the MM2\* results are considered. In particular, AMBER\* overestimates the exclusive H-2–H-1 and H-4–H-1 NOEs, which probably means that the actual population around minimum *anti* is smaller than that calculated, 49%, and closer to that calculated by MM2\* (around 15%). The H-3–H-1' intensity is fairly well reproduced by both force fields, especially by MM2\*. Therefore, the experimental NOEs could be explained by a population distribution similar to that proposed by MM2\*, with the *syn* and *anti* regions populated in about 80–85 and 15–20%, respectively. A clear increase in the population of the *anti* region is evident when the interglycosidic oxygen is substituted by sulfur. Similar results have been recently described for other thio-oligosaccharides [18–20].

In conclusion, both compounds present a conformational equilibrium in solution between two major regions. In the case of the natural compound, **1**, one of these is heavily populated (ca. 95%). Nevertheless, the glycosidic linkages still present certain flexibility. In the case of the thio analogue **2**, the *syn* region is still dominant, although the *anti* conformer is clearly present (ca. 15–20%). This increase of flexibility could probably be due to the fact that the C–S bond is longer than the C–O analogue, and fewer steric conflicts occur for the *anti* conformation. It has also to be considered that the C–S–C bond angle is ca. 98° compared to ca. 117° for C–O–C. According to the observed populations, the change in relative energy is smaller than 1 kcal/mol. From the point of view of the molecular recognition of these sugars by a natural receptor, it seems that the global three-dimensional shape of both compounds in solution is fairly similar, and therefore the thio disaccharide could be chosen as a mimic of the natural compound, especially for studying interactions with enzymes that may destroy *O*-glycosidic linkages, but that cannot affect the *S*-glycosidic linkages.

### 3. Experimental

**General Methods.**—Melting points are uncorrected. TLC was performed using TLC plates GF<sub>254</sub> with detection by charring with 5% H<sub>2</sub>SO<sub>4</sub> in EtOH. Column chromatography was performed on silica gel (230–400 mesh). The eluent used is indicated and solvent ratios refer to volume. Solvents were distilled over drying agents: dimethylformamide (DMF), BaO; dichloromethane (DCM), CaH<sub>2</sub>; acetonitrile (MeCN), CaH<sub>2</sub>. <sup>1</sup>H NMR spectra were registered at 500 or 300 Mz. <sup>13</sup>C NMR spectra were obtained at 125 or 50 MHz.

**Allyl 2-acetamido-3,4,6-tri-O-acetyl-2-deoxy-β-D-glucopyranoside (4).**—To a solution of 2-acetamido-1,3,4,6-tri-O-acetyl-2-deoxy-α-D-glucopyranose (**3**) (11.7 g, 30 mmol) and AlOH (6.1 mL, 90 mmol) in MeCN (100 mL) under argon, was added 4 Å molecular sieves (5 g). After 10 min, SnCl<sub>4</sub> (4.2 mL, 36 mmol) was added dropwise, and the mixture was stirred at 70 °C for 8 h. After cooling, the mixture was neutralized with triethylamine, filtered through a pad of celite and concentrated. The residue was purified by column chromatography (1:2 hexane–EtOAc) to give 2-acetamido-3,4,6-tri-O-acetyl-2-deoxy-α-D-glucopyranoside (1.39 g, 12%) and then **4** (5.6 g, 49%) as a white solid, mp 163–165 °C (lit 164–167 °C [21]). [α]<sub>D</sub> –13.8° (c 1, CHCl<sub>3</sub>) (lit. –14.4° [21]). <sup>1</sup>H NMR (CDCl<sub>3</sub>, 300 MHz): δ 5.92–5.79 (m, 1 H, –CH=CH<sub>2</sub>), 5.62 (d, 1 H, J<sub>NH,2</sub> 8.8 Hz, NH), 5.30 (dd, 1 H, J<sub>3,4</sub> 9.4 Hz, J<sub>2,3</sub> 10.6 Hz, H-3), 5.25–5.17 (m, 2 H, –CH=CH<sub>2</sub>), 5.07 (t, 1 H, J<sub>3,4</sub> ≈ J<sub>4,5</sub> 9.5 Hz, H-4), 4.71 (d, 1 H, J<sub>1,2</sub> 8.3 Hz, H-1), 4.37–4.30 (m, 1 H, OCH<sub>2</sub>–CH=), 4.26 (dd, 1 H, J<sub>5,6a</sub> 4.7 Hz, J<sub>6a,6b</sub> 12.2 Hz, H-6a), 4.13 (dd, 1 H, J<sub>5,6b</sub> 2.4 Hz, J<sub>6a,6b</sub> 12.2 Hz, H-6b), 3.88 (dt, 1 H, J<sub>2,NH</sub> ≈ J<sub>1,2</sub> 8.6 Hz, J<sub>2,3</sub> 10.6 Hz, H-2), 3.72–3.67 (m, 1 H, H-5), 2.08 (s, 3 H, Me), 2.03 (s, 3 H, Me), 2.02 (s, 3 H, Me), 1.95 (s, 3 H, Me). <sup>13</sup>C NMR (CDCl<sub>3</sub>, 50 MHz): δ 170.75 (CO), 172.62 (CO), 170.23 (CO), 169.33 (CO), 133.57 (–CH=CH<sub>2</sub>), 117.59 (–CH=CH<sub>2</sub>), 99.65 (C-1), 72.41, 71.72, 69.86 (OCH<sub>2</sub>–CH=), 68.78, 62.19 (C-6), 54.63 (C-2), 23.19 (Me), 20.64 (Me), 20.60 (Me), 20.53 (Me).

**Allyl 2-acetamido-4,6-O-benzylidene-2-deoxy-β-D-glucopyranoside (5).**—Compound **4** (1.43 g, 3.71 mmol) was treated with a solution of NaOMe in MeOH (0.1M, 140 mL) at r.t. for 1 h. After this time, the reaction mixture was neutralized with Amberlita IR-120 (H<sup>+</sup>), and filtered. The solvent was evaporated, and the crude was suspended in

MeCN (23 mL) and treated with PhCH(OMe)<sub>2</sub> (2.77 mL, 11.5 mmol) and *p*-TsOH·H<sub>2</sub>O (35.3 mg, 0.18 mmol) at r.t. for 2 h. Then, the mixture was diluted with dichloromethane (50 mL), neutralized with triethylamine and concentrated. The residue was purified by column chromatography (40:1→20:1 DCM–MeOH) to give **5** (1.17 g, 91%) as a white solid, mp 279–282 °C (dec) (lit, 279–281 °C (dec) [22]). <sup>1</sup>H NMR (CDCl<sub>3</sub>, 300 MHz): δ 7.35–7.52 (m, 5 H, Ar), 5.85–5.92 (m, 1 H, OCH<sub>2</sub>–CH=), 5.71 (d, 1 H, *J*<sub>NH,2</sub> 5.7 Hz, NH), 5.57 (s, 1 H, CHPh), 5.24–5.36 (m, 2 H, –CH=CH<sub>2</sub>), 4.78 (d, 1 H, *J*<sub>1,2</sub> 8.3 Hz, H-1), 4.33–4.41 (m, 2 H, OCH<sub>2</sub>–CH=, H-6e), 4.20 (t, 1 H, *J*<sub>2,3</sub>≈*J*<sub>3,4</sub> 9.5 Hz, H-3), 4.07–4.15 (m, 1 H, OCH<sub>2</sub>–CH=), 3.81 (t, 1 H, *J*<sub>5,6a</sub>≈*J*<sub>6a,6b</sub> 9.8 Hz, H-6a), 3.59 (t, 1 H, *J*<sub>3,4</sub>≈*J*<sub>4,5</sub> 9.4 Hz, H-4), 3.44–3.54 (m, 2 H, H-2, H-5), 2.06 (s, 3 H, Me). <sup>13</sup>C NMR (CDCl<sub>3</sub>–CD<sub>3</sub>OD 7:1, 50 MHz): δ 172.33 (CO), 136.92 (C-*ipso*), 133.48 (–CH=CH<sub>2</sub>), 129.04, 128.09, 126.11 (Ar), 117.34 (–CH=CH<sub>2</sub>), 101.65 (CHPh), 100.20 (C-1), 81.49, 70.03, 68.47, 66.09, 57.26 (C-2), 22.74 (Me).

*Allyl O*-(2,3,4-*tri-O*-benzyl- $\alpha$ -L-fucopyranosyl)-(1→3)-2-acetamido-4,6-*O*-benzylidene-2-deoxy- $\beta$ -D-glucopyranoside (**7**).—Ethyl 2,3,4-*tri-O*-benzyl-1-thio- $\beta$ -L-fucopyranoside [8] (430 mg, 0.9 mmol) was dissolved in dichloromethane (6.5 mL) under argon. At 0 °C, bromine (47.3 mL, 0.91 mmol) was added and the mixture was stirred for 30 min. The mixture was concentrated in vacuo and residual bromine was removed by evaporation with toluene (3×10 mL), to give crude bromide **6**. Acceptor **2** (209 mg, 0.6 mmol) was dissolved in DMF (5.5 mL) and 4 Å molecular sieves and Bu<sub>4</sub>NBr (193.4 mg, 0.6 mmol) were added. The mixture was kept under an argon atmosphere and bromide **6** (0.9 mmol) dissolved in dichloromethane (1 mL) was added. After stirring for 18 h, the reaction was quenched with ethanol. After 30 min, the mixture was diluted with dichloromethane and filtered through a pad of celite. The filtrate was washed with saturated aqueous NaHCO<sub>3</sub>, brine, dried (Na<sub>2</sub>SO<sub>4</sub>) and concentrated in vacuo. The residue was purified by column chromatography (2:1 hexane–EtOAc) to give **7** (361 mg, 79%) as a white solid, mp 82–85 °C, [ $\alpha$ ]<sub>D</sub> –84.5° (*c* 1, CHCl<sub>3</sub>). <sup>1</sup>H NMR (CDCl<sub>3</sub>, 300 MHz): δ 7.17–7.47 (m, 15 H, Ar), 5.75–5.86 (m, 1 H, –CH=CH<sub>2</sub>), 5.63 (d, 1 H, *J*<sub>NH,2</sub> 7.1 Hz, NH), 5.49 (s, 1 H, CHPh), 5.14–5.28 (m, 2 H, –CH=CH<sub>2</sub>), 5.05 (d, 1 H, *J*<sub>1',2'</sub> 3.4 Hz, H-1'), 4.55–4.93 (m, 7 H, 3 CH<sub>2</sub>Ph, H-1), 4.25–4.35 (m, 3 H, H-6e, H3, OCH<sub>2</sub>–CH=), 4.01–4.08 (m, 3 H, H-2',

H-5', OCH<sub>2</sub>–CH=), 3.93 (dd, 1 H, *J*<sub>3',4'</sub> 2.6 Hz, *J*<sub>2',3'</sub> 10.0 Hz, H-3'), 3.75 (t, 1 H, *J*<sub>5,6a</sub>≈*J*<sub>6a,6e</sub> 10.0 Hz, H-6a), 3.36–3.59 (m, 4 H, H-2, H-4, H-5, H-4'), 1.6 (s, 3 H, Me), 0.8 (d, 3 H, *J*<sub>Me,5'</sub> 6.3 Hz, Me-Fuc). <sup>13</sup>C NMR (CDCl<sub>3</sub>, 50 MHz): δ 170.47 (CO), 138.61 (C-*ipso*), 138.54 (C-*ipso*), 137.28 (C-*ipso*), 133.71 (–CH=CH<sub>2</sub>), 128.98, 128.60, 128.38, 128.22, 128.16, 127.86, 127.71, 127.64, 127.28, 126.19 (Ar), 117.57 (–CH=CH<sub>2</sub>), 101.58 (CHPh), 99.91 (C-1), 98.33 (C1'), 80.81, 79.82, 77.64, 76.37, 74.88, 74.16, 72.51, 70.26, 68.81, 66.86, 66.19, 58.27 (C-2), 23.21 (Me), 16.27 (Me-Fuc). Anal. Calcd for C<sub>45</sub>H<sub>51</sub>NO<sub>10</sub>: C, 70.57; H, 6.71; N, 1.83. Found: C, 70.27; H, 6.80; N, 1.92.

*Propyl O*-( $\alpha$ -L-fucopyranosyl)-(1→3)-2-acetamido-2-deoxy- $\beta$ -D-glucopyranoside (**1**).—A solution of **7** (90 mg, 0.117 mmol) in MeOH (25 mL) and EtOAc (5 mL) was added Pd/C (250 mg) and the mixture was stirred under H<sub>2</sub> atmosphere for 4.5 h. After this time, the reaction mixture was filtered through a pad of celite, and concentrated. The residue was purified by column chromatography (4:1 DCM–MeOH) to give **1** (46 mg, 96%), mp 228–231 °C (dec). [ $\alpha$ ]<sub>D</sub> –112.6° (*c* 0.68, MeOH). <sup>1</sup>H NMR (D<sub>2</sub>O, 500 MHz): δ 4.98 (d, 1 H, *J*<sub>1',2'</sub> 4.1 Hz, H-1'), 4.53 (d, 1 H, *J*<sub>1,2</sub> 8.7 Hz, H-1), 4.33 (m, 1 H, H-5'), 3.93 (dd, 1 H, *J*<sub>5,6a</sub> 2.3 Hz, *J*<sub>6a,6b</sub> 12.3 Hz, H-6a), 3.86–3.78 (m, 4 H, OCH, H-3', H-4', H-2), 3.76 (dd, 1 H, *J*<sub>5,6b</sub> 5.6 Hz, *J*<sub>6a,6b</sub> 12.3 Hz, H-6b), 3.70 (dd, 1 H, *J*<sub>1',2'</sub> 4.1 Hz, *J*<sub>2',3'</sub> 10.5 Hz, H-2'), 3.64 (t, 1 H, *J*<sub>2,3</sub>≈*J*<sub>3,4</sub> 8.5 Hz, H-3), 3.57 (m, 1 H, OCH), 3.52 (dd, 1 H, *J*<sub>3,4</sub> 8.5 Hz, *J*<sub>4,5</sub> 8.9 Hz, H-4), 3.45 (m, 1 H, H-5), 1.81 (s, 3 H, Me), 1.33 (m, 2 H, CH<sub>2</sub>), 0.94 (d, 1 H, *J*<sub>Me,5'</sub> 6.7 Hz, Me-Fuc), 0.65 (t, *J* 7.3 Hz, Me). <sup>13</sup>C NMR (D<sub>2</sub>O, 125 MHz): δ 175.56 (CO), 101.85 (C-1), 100.88 (C-1'), 81.43, 76.86, 73.31 (OCH<sub>2</sub>), 72.83, 70.54, 69.62, 68.98, 67.89, 61.80 (C-6), 56.3 (C-2), 23.17 (Me), 23.06 (CH<sub>2</sub>), 16.16 (Me-Fuc), 10.56 (Me). Anal. Calcd for C<sub>17</sub>H<sub>31</sub>NO<sub>10</sub>: C, 49.87; H, 7.63; N, 3.42. Found: C, 49.54; H, 7.51; N, 3.40.

#### 4. Conformational calculations: molecular mechanics

Glycosidic torsion angles are defined as  $\phi$  H-1'–C-1'–O(S)–C-3 and  $\psi$  C-1'–O(S)–C-3–H-3 for both analogues. This convention is related to that which employs heavy atoms (O-5 for  $\Phi$  and C-4 for  $\Psi$ ) by adding 120°. The reducing end was considered to be  $\beta$ -*O*-methylated for the sake of simplicity.

Relaxed ( $\phi$ ,  $\psi$ ) potential energy maps were calculated using MM3\* (MM2\* for the *S*-analogue due to the lack of parameters of MM3\* for sulfur) and AMBER\* force fields as implemented in MACROMODEL 4.5 [23], with dielectric constant  $E = 80$ . These MACROMODEL force fields differ from the regular force fields in the treatment of the electrostatics since they employ charge–charge instead of dipole–dipole interactions. The AMBER\* force field uses Homans parameters for carbohydrates [24].

All calculations were made for the  $\beta$ -*O*-methyl anomer of GlcNAc. Four initial geometries were considered: cc, cr, rr and rc, obtained by combining the positions r (reverse clockwise) and c (clockwise) for the orientation of the secondary hydroxyl groups of both pyranoid moieties. The first character corresponds to the non-reducing fucose moiety, and the second one, to the GlcNAc. The *gauche*–*trans* rotamer [25] of the GlcNAc moiety was considered for the  $\omega$  torsion angle (O-5–C-5–C-6–O-6), as  $+60^\circ$ . Four relaxed energy maps were obtained following a similar protocol to that described previously [13]. A grid search of  $18^\circ$  was employed for the generation of the potential energy surfaces. Adiabatic surfaces [10,11] were built, and the probability distributions calculated for each  $\phi, \psi$  point according to a Boltzmann function.

## 5. NMR experiments

NMR spectra of both derivatives were recorded at 310 K in  $D_2O$ , using a Varian Unity 500 MHz spectrometer. Proton chemical shifts were referenced to residual HDO at  $\delta$  4.64 ppm. COSY and TOCSY spectra permitted the assignment of the proton spin systems. Selective 1D double pulse field gradient spin echo experiments [26] were recorded for both sugars using four different mixing times, namely 150, 300, 450, and 600 ms. Only the data at 300 and 450 ms are shown.

## 6. NOE calculations

NOESY spectra were simulated according to a complete relaxation matrix approach, following the protocol previously described [13], using four different mixing times (between 150 and 600 ms). Different mixing times were used in order to eval-

uate the influence of three spin effects. At short mixing times, multispin effects are fairly negligible but NOEs are small. At longer mixing times, the multispin effect becomes relevant but NOEs are stronger and easy to measure [17]. The spectra were simulated from the average distances  $\langle r^{-6} \rangle_{kl}$  calculated from the relaxed energy maps at 310 K. Isotropic motion and external relaxation of  $0.1 \text{ s}^{-1}$  were assumed. A  $\tau_c$  of 45 ps was used to obtain the best match between experimental and calculated NOEs for two given intraresidue proton pairs (H-1'–H-2' and H-5'–H-3' + H-4').

All the NOE calculations were automatically performed by a home-made program, available from the authors upon request [13].

## Acknowledgements

The authors thank DGICYT (Grant PB96-0833) and the Mizutani Glycoscience Foundation for financial support. B.A. is grateful to the Ministerio de Educación y Cultura for a fellowship.

## References

- [1] L.A. Lasky, *Science*, 258 (1992) 964–969.
- [2] K. Fukushima, M. Hirota, P.I. Terasaki, A. Wakisaka, H. Togashi, D. Chia, N. Suyama, Y. Fukushi, E. Nudelman, and S. Hakomori, *Cancer Res.*, 44 (1984) 5279–5285.
- [3] F.F. Santos-Benito, A. Fernández-Mayoralas, M. Martín-Lomas, and M. Nieto-Sampedro, *J. Exp. Med.*, 176 (1992) 915–918; J.M. Coterón, S. Kamaljit, J.L. Asensio, M. Domínguez-Dalda, A. Fernández-Mayoralas, J. Jiménez-Barbero, M. Martín-Lomas, J. Abad-Rodríguez, and M. Nieto-Sampedro, *J. Org. Chem.*, 60 (1995) 1502–1519; M. Nieto-Sampedro, C. Bailón, A. Fernández-Mayoralas, M. Martín-Lomas, B. Mellstrom, and J.R. Naranjo, *J. Neuropath. Exp. Neur.*, 55 (1996) 169–177.
- [4] J. Defaye and J. Gelas, in Atta-ur-Rahman (Ed.), *Studies in Natural Products Chemistry*, Vol. 8, Elsevier, Amsterdam, 1991, pp 315–357; H. Dri-guez, *Top. Curr. Chem.*, 187 (1997) 85–116.
- [5] T. Peters and B.M. Pinto, *Curr. Opin. Struct. Biol.*, 6 (1996) 710–716.
- [6] A. Imberty, *Curr. Opin. Struct. Biol.*, 7 (1997) 617–623.
- [7] S.S. Rana, J.J. Barlow, and K.L. Matta, *Carbo-hydr. Res.*, 91 (1981) 149–157; B.M. Heskamp, G.H. Veeneman, G.A. van der Marel, C.A.A. van

- Boeckel, and J.H. van Boom, *Recl. Trav. Chim. Pays-Bas*, 114 (1995) 398–402.
- [8] H. Lohn, *Carbohydr. Res.*, 139 (1985) 105–113.
- [9] B. Aguilera, A. Fernández-Mayoralas, and C. Jaramillo, *Tetrahedron*, 53 (1997) 5863–5876.
- [10] A. French and J.W. Brady (Eds.), *Computer Modeling of Carbohydrate Molecules*, ACS Symp. Ser. 430 (1990).
- [11] M. Martín-Pastor, J.F. Espinosa, J.L. Asensio, and J. Jiménez-Barbero, *Carbohydr. Res.*, 298 (1997) 15–49.
- [12] J. Dabrowski, T. Kozár, H. Grosskurth, and N. E Nifant'ev, *J. Am. Chem. Soc.*, 117 (1995) 5534–5539.
- [13] J.L. Asensio and J. Jiménez-Barbero, *Biopolymers*, 35 (1995) 55–73.
- [14] H. Thogersen, R.U. Lemieux, K. Bock, and B. Meyer, *Can. J. Chem.*, 60 (1982) 44–57.
- [15] A. Imberty, E. Mikros, J. Koca, R. Mollicone, R. Oriol, and S. Perez, *Glycoconjugate J.*, 12 (1995) 331–349.
- [16] S. Perez, N. Mouhous-Riou, N.E. Nifant'ev, Y.E Tsvetkov, B. Bachet, and A. Imberty, *Glycobiology*, 6 (1996) 537–542.
- [17] D. Neuhaus and M.P. Williamson, *The Nuclear Overhauser Effect in Structural and Conformational Analysis*, VCH, New York, 1989.
- [18] K. Bock, J.O. Duus, and S. Refn, *Carbohydr. Res.*, 253 (1994) 51–67.
- [19] A. Geyer, G. Hummel, T. Eisele, S. Reinhardt, and R.R. Schmidt, *Chem. Eur. J.*, 2 (1996) 981–988.
- [20] U. Nilsson, R. Johansson, and G. Magnusson, *Chem. Eur. J.*, 2 (1996) 295–302.
- [21] M. Kiso and L. Anderson, *Carbohydr. Res.*, 72 (1979) C12–C14.
- [22] M.A.E. Shaban, V.N. Reinhold, and R.W. Jeanloz, *Carbohydr. Res.*, 55 (1977) 213–233.
- [23] F. Mohamadi, N.G.J. Richards, W.C. Guida, R. LisKamp, C. Caufield, G. Chang, T. Hendrickson, and W.C. Still, *J. Comput. Chem.*, 11 (1990) 440–467.
- [24] S.W. Homans, *Biochemistry*, 29 (1990) 9110–9118.
- [25] K. Bock and J. Duus, *J. Carbohydr. Chem.*, 13 (1993) 513–543.
- [26] K. Stott, J. Stonehouse, J. Keeler, T.L. Hwang, and A.J. Shaka, *J. Am. Chem. Soc.*, 117 (1995) 4199–4200.